Control Engineering Practice ∎ (∎∎∎∎) ∎∎∎–∎∎∎

Contents lists available at ScienceDirect

Control Engineering Practice

journal homepage: www.elsevier.com/locate/conengprac

Fault tolerant control of a simulated hydroelectric system ☆

Q1 Silvio Simani *, Stefano Alvisi, Mauro Venturini

Dipartimento di Ingegneria, Università degli Studi di Ferrara. Via Saragat 1E, 44122 Ferrara, FE, Italy

ARTICLE INFO

Article history:
Received 31 July 2015
Received in revised form
14 March 2016
Accepted 15 March 2016

Keywords:
Fault tolerant control
Control design
Modelling and identification
Adaptive control
Hydraulic system

ABSTRACT

This paper analyses the application of two fault tolerant control schemes to a hydroelectric model developed in the Matlab and Simulink environments. The proposed fault tolerant controllers are exploited for regulating the speed of the Francis turbine included in the hydraulic system. The nonlinear behaviour of the hydraulic turbine and the inelastic water hammer effects are taken into account in order to develop a high-fidelity simulator of this dynamic plant. The first fault tolerant control solution relies on an adaptive control design, which exploits the recursive identification of a linear parametric time-varying model of the monitored system. The second scheme proposed uses the identification of a fuzzy model that is exploited for the reconstruction of the fault affecting the system under diagnosis. In this way, the fault estimation and its accommodation is possible. Note that these strategies, which are both based on identification approaches, are suggested for enhancing the application of the suggested fault tolerant control methodologies. These characteristics of the study represent key issues when on-line implementations are considered for a viable application of the proposed fault tolerant control schemes. The faults considered in this paper affect the electric servomotor used as a governor, the hydraulic turbine speed sensor, and the hydraulic turbine system, and are imposed both separately and simultaneously. Moreover, the complete drop of the rotational speed sensor is also analysed. Monte-Carlo simulations are also used for analysing the most important issues of the proposed schemes in the presence of parameter variations. Moreover, the performances achieved by means of the proposed solutions are compared to those of a standard PID controller already developed for the considered model. Finally, these strategies serve to highlight the potential application of the proposed control strategies to real hydraulic systems.
© 2016 Published by Elsevier Ltd.

UNCORRECTED PROOF

1. Introduction

Modern technological and technical processes are based on complex control systems that are designed to meet advanced performance and safety requirements. Conventional feedback control solutions may lead to unsatisfactory performances, or even to instability, when possible malfunctions in actuators, sensors or other system components are present. To overcome these problems, new strategies to control system design have been proposed in order to manage actuator, sensor and component faults, while maintaining desirable stability and performance properties. This class of control design is also known as Fault Tolerant Control (FTC) systems, which have the capability to accommodate the faults in an automatic way. The closed-loop control system is thus able to manage any malfunctions, while maintaining good control properties. The FTC system is based on adaptive strategies or active Fault Detection and Diagnosis (FDD) scheme, *i.e.* when the fault function is estimated and compensated. Regarding the latest issue, many FDD techniques have been developed, see for example the survey works (Chen & Patton, 1999; Ding, 2008).

Q2 In general, FTC solutions are divided into two strategies, namely Passive Fault Tolerant Control Scheme (PFTCS) and Active Fault Tolerant Control Scheme (AFTCS), as addressed *e.g.* in Blanke, Kinnaert, Lunze, and Staroswiecki (2006), Zhang and Jiang (2008), and Noura, Theilliol, Ponsart, and Chamseddine (2009). On one hand, in the case of PFTCS, the designed controllers are defined and designed to be robust with respect to a specific set of presumed faults. This scheme uses neither FDD methods nor controller reconfiguration, but it presents limited fault tolerant features (Zhang & Jiang, 2008). On the other hand, AFTCS reacts actively to the system fault by using a control accommodation approach, so that the stability and the final performance of the entire system are maintained. Concerning AFTCS, it was remarked that robust and reliable FDD are required (Chen & Patton, 1999; Ding, 2008).

FTC solutions can derive from the application of model-based and model-free designs, as described *e.g.* in Blanke et al. (2006)

☆Invited paper for the special issue on "Industrial Practice of Fault Diagnosis and Fault Tolerant Control" organised by Peter Fogh Odgaard.

* Corresponding author.
E-mail addresses: silvio.simani@unife.it (S. Simani), stefano.alvisi@unife.it (S. Alvisi), mauro.venturini@unife.it (M. Venturini).
URL: http://www.silviosimani.it (S. Simani).

http://dx.doi.org/10.1016/j.conengprac.2016.03.010
0967-0661/© 2016 Published by Elsevier Ltd.

and Zhang and Jiang (2008). Different FTC methods have been addressed in the recent related literature. For example, Kim and Kim (2015) proposed stochastic petri nets exploited for designing process control system of a continuous casting plant. The work of Schuh, Zgorzelski, and Lunze (2015) presented deterministic input/output automata applied to a handling system. The paper by Fonod et al. (2015) developed a control system to detect, isolate and accommodate single faults affecting the thruster-based propulsion system of an autonomous spacecraft. Ubaid, Daley, and Pope (2015) described a control design procedure through its application to a laboratory scale slab floor. The study of Li, Liu, and Cao (2015) presented a robust H_∞ approach used to solve an optimal state-feedback-type controller parameter design for a HVDC/AC system. The paper by Kiltz, Join, Mboup, and Rudolph (2014) introduced a method based on algebraic derivative estimation that is applied on an example of electromagnetically supported plate. Finally, the work of Blesa, Rotondo, Puig, and Nejjari (2014) used interval observers oriented to the design of virtual sensors/actuators for wind turbines.

On the other hand, few works analysed the model-based fault tolerant control problem when applied to hydroelectric plants, as described in Hong, Guangda, and Weiyou (2008), Li et al. (1992), and Wei, Wei-bo, Gen-mao, and Jian-hua (2000). In fact, as a mathematical model is needed for the description of the system behaviour, precise modelling for these processes could be difficult to achieve in practice. There are several works that discuss the modelling of hydroelectric processes with their controller design, as in Mansoor, Jones, Bradley, Aris, and Jones (2000) and Weber, Prillwitz, Hladky, and Asal (2001). These works consider the elastic water effects, though the nonlinear dynamics are linearised at an operating point. Other papers (Eker, 2004; Hanmandlu & Goyal, 2008; Kishor, Saini, & Singh, 2007) considered different mathematical descriptions with the techniques to control the power systems. Moreover, linear and nonlinear plants with various water column effects and control solutions are also considered. Mahmoud, Dutton, and Denman (2005) and Kishor, Singh, and Raghuvanshi (2006) addressed complex control solutions for hydraulic processes.

In some cases, it could be impossible to describe the nonlinear systems in an analytical way; moreover, the system structure with its parameters and measurements can be almost unknown. Therefore, parametric model estimation can represent an alternative solution for deriving practical models of nonlinear dynamic processes systems for control design. Moreover, if nonlinear identification methods require a detailed knowledge of the model structure, fuzzy systems and neural networks can be obtained directly from measured data (Alvisi & Franchini, 2012; Asgari, Venturini, Chen, & Sainudiin, 2014; Nelles, 2001).

This paper proposes two fault-tolerant control approaches for the adjustment of a hydraulic turbine developed in the Matlab® and Simulink® environments. The development of the suggested solutions is particularly important from a practical point of view. In fact, the variable demand for electricity and changing conditions in the power system can lead to different demand of peak energy generation, with short response time and fast frequency changes. Hydroelectric power systems thus require to operate taking into account different variable load and demand conditions. In general, the operation of hydropower systems can frequently experience variations in the flow in both routine operations and abnormal conditions. In particular, turbine operations such as start-up, load acceptance, load rejection and shutdown can lead to hydraulic transients that can generate large pressure and sub-pressure oscillations, which must be carefully evaluated to avoid mechanical failures in the hydraulic systems. Therefore, the need for accurate simulation of transient flow in hydroelectric power plants is obvious. However, even if the basic technology in a hydraulic process has not changed much, powerful computers and software now can be used to provide virtual models and simulators of hydropower systems.

Therefore, this work proposes a first methodology based on the fuzzy theory, as it represents a suitable method to manage almost unknown situations and uncertain measurements (Babuška, 1998). In this way, instead of using purely nonlinear analytical description obtained via the first principle modelling approach, the paper proposes to exploit Takagi–Sugeno (TS) models (Babuška, 1998; Takagi & Sugeno, 1985), whose parameters are estimated via an identification methodology. In particular, the fuzzy fault tolerant scheme is obtained according to the following stages. The FDD model is firstly estimated using the fuzzy identification approach (Babuška, 1998). Secondly, the fault accommodation strategy uses the estimation of FDD module to compensate for the fault effect. The FDD model is obtained via a proper choice of the fuzzy model parameters. The Membership Functions (MFs) with their rules are also derived directly from the data of the monitored system. The fuzzy modelling and identification scheme is thus able to lead to the required fault tolerance features. Note that the proposed design approach exploited for the derivation of the fuzzy controller was already addressed in Simani and Castaldi (2013), but applied to a wind turbine system, and without fault tolerance capabilities.

Concerning the traditional controller design, classical linear control schemes, such as the PID solution could not lead to satisfactory behaviour for all operating points of the plant, due to nonlinearity, system ageing, environmental conditions, uncertain measurements, disturbance and possible faults. Due to this behaviour, possible solutions could exploit a multiple model approach, or gain-scheduled controllers that are derived to work in fixed operating points, as described *e.g.* in Fang, Chen, Dlakavu, and Shen (2008). In this case, it was assumed that the model parameters change slowly compared to the system dynamics, which is generally not satisfied. Moreover, classic gain-scheduling strategies could guarantee prescribed performance and stability requirements at different operating points, but with design procedures that sometimes are not direct and straightforward.

Under these considerations, the second FTC approach suggested in this paper uses a recursive identification mechanism in connection with model-based adaptive control design, which was addressed *e.g.* in Bobál, Böhm, Fessl, and Machácek (2005). Note that this alternative strategy suggested in this paper for the adaptive controller design was already proposed in Simani, Alvisi, and Venturini (2014), but without any fault tolerance properties. Therefore, the controller design problem is proposed here since the characteristics of the process under investigation can change over time. Moreover, in the perspective of the fault tolerant application, this paper suggests to exploit an *adaptive* solution based on a recursive or on-line estimation scheme relying on the on-line estimation of the controlled process, which is affected by faults. While the time-varying parameters of the plant are identified, which are the result of both disturbance and faults, the time-varying variables of the controller are computed on-line, in order to maintain fixed control performances.

The efficacy of the suggested FTC strategies are proved on different data sequences acquired from the hydraulic system under diagnosis. Several simulations provide the effectiveness of the proposed regulators also with respect to the baseline PID controller proposed in Fang et al. (2008), when both the fault tolerance and the reference tracking capabilities are considered. Moreover, as it fundamental to analyse the behaviour of the proposed control strategies with respect to modelling uncertainties, the suggested verification tool exploits extensive Monte-Carlo simulations. In fact, as the hydraulic plant uses a hydraulic turbine represented as two-dimensional map, the Monte-Carlo analysis represents a viable approach for assessing the performances of the

UNCORRECTED PROOF

Please cite this article as: Simani, S., et al. Fault tolerant control of a simulated hydroelectric system. *Control Engineering Practice* (2016), http://dx.doi.org/10.1016/j.conengprac.2016.03.010

suggested fault tolerant control schemes.

The paper has the following structure. Section 2 briefly recalls the model of the hydraulic system. Section 3 sketches the suggested FTC design solutions, which rely on both the fuzzy modelling and identification strategy exploited here for obtaining the input–output description of the considered simulated process and the FDD module for fault estimation and compensation. The second adaptive approach is also recalled in Section 3. The obtained results are described in Section 4, which shows the simulations from the developed FTC schemes, assessed and compared with respect to the classic PID regulator. Finally, Section 5 highlights the main achievements of the paper, by suggesting also open problems and further investigations.

2. Hydraulic system and fault modes

2.1. Hydraulic system model

The simulated hydroelectric power plant considered in this work is represented in Fig. 1 (Fang et al., 2008; Simani, Alvisi, et al., 2014; Simani, Alvisi, & Venturini, 2015).

It consists of a reservoir with constant water level H_R, an upstream water tunnel with cross-section area A_1 and length L_1, an upstream surge tank with cross-section area A_2, and water level H_2. This is followed by a downstream surge tank with cross-section area A_4 and water level H_4, and a downstream tail water tunnel with cross-section area A_5 and length L_5. Moreover, the penstock between hydraulic turbine and two surge tanks has a cross-section area A_3 and length L_3. T denotes the hydraulic turbine. Finally, a tail water lake has constant water level H_T.

The expressions (1) and (2) represent the non-dimensional flow rate and water pressure in terms of the corresponding relative deviations:

$$\frac{Q}{Q_r} = 1 + q \tag{1}$$

$$\frac{H}{H_r} = 1 + h \tag{2}$$

where Q is the water flow rate, Q_r is the rated flow rate, q is the flow rate relative deviation, whilst H is the water pressure, H_r is the rated water pressure, and h the water pressure relative deviation.

According to Fang et al. (2008), with reference to a pressure water supply system, Newton's second law for a fluid element inside a tube and the conservation mass law for a control volume, which accounts for water compressibility and tube elasticity, is written. Under the assumption that the penstock is short or medium in length, water and pipeline is considered incompressible and rigid, respectively. Therefore, (3) considers only the inelastic water hammer effect (Fang et al., 2008):

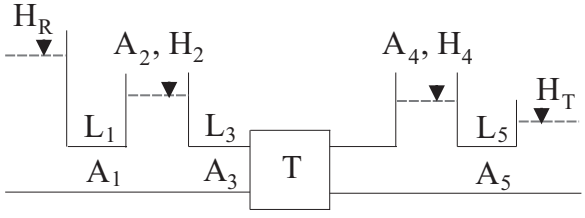

Fig. 1. Layout of the simulated hydropower plant.

$$\frac{h}{q} = -T_w s - H_f \tag{3}$$

where s is the derivative operator. Under this assumption, the expression (3) represents the flow rate deviation and the water pressure deviation transfer functions for a simple penstock, where H_f is the hydraulic loss and T_w is the water inertia time:

$$T_w = \frac{L\,Q_r}{g\,A\,H_r} \tag{4}$$

depending on the penstock length L, the rated flow rate Q_r, the gravity acceleration g, the cross-section area A, and the rated water pressure H_r. The hydroelectric power plant considered in this work is divided into three sections: the upstream water tunnel, the penstock and the downstream tail water tunnel.

The upstream water tunnel connects the reservoir to the upstream surge tank. Since the inlet of upstream water tunnel is in reservoir and the water pressure deviation of the inlet is constant during hydraulic transients, the transfer function of the flow rate deviation and the water pressure deviation of the outlet of the upstream water tunnel is expressed in the form:

$$\frac{h_1}{q_1} = -T_{w_1} s - H_{f_1} \tag{5}$$

The downstream tail water tunnel connects the downstream surge tank to the tail water lake. It is assumed that the outlet of the downstream tail water tunnel is in tailwater lake and the water pressure deviation of the outlet is constant. Therefore, the transfer function of flow rate deviation and the water pressure deviation of the inlet of downstream tail water tunnel has the form:

$$\frac{h_5}{q_5} = -T_{w_5} s - H_{f_5} \tag{6}$$

Usually, the water inertia in the draft tube is considered within the penstock. Thus, the transfer function of flow rate deviation (the subscript t refers to the turbine) and the water pressure deviation of the penstock is written as:

$$h_t = h_2 - h_4 + h_3 \tag{7}$$

where:

$$\frac{h_3}{q_3} = -T_{w_3} s - H_{f_3} \tag{8}$$

The expressions of the surge tanks are derived from the continuity of flow at the two junctions, where the hydraulic losses at orifices of surge tanks are neglected:

$$\begin{cases} \dfrac{A_2\,H_r}{Q_r}\dfrac{dh_2}{dt} = q_2 = q_1 - q_3 \\ \dfrac{A_4\,H_r}{Q_r}\dfrac{dh_4}{dt} = q_4 = q_3 - q_5 \end{cases} \tag{9}$$

The surge tank filling time is expressed as:

$$T_s = \frac{A\,H_r}{Q_r} \tag{10}$$

Regarding the Francis turbine in Fig. 1, according to Simani, Alvisi, et al. (2014), the second order polynomial curve (11) relates the non-dimensional water flow rate Q/Q_r to the non-dimensional rotational speed n/n_r. The non-dimensional parameter G (varying in the range between 0 and 100%) represents the turbine wicked gate opening:

$$\frac{Q}{Q_r} = G\left[a_1\left(\frac{n}{n_r}\right)^2 + b_1\left(\frac{n}{n_r}\right) + c_1\right] = f_1(n, G) \tag{11}$$

UNCORRECTED PROOF

Please cite this article as: Simani, S., et al. Fault tolerant control of a simulated hydroelectric system. *Control Engineering Practice* (2016), http://dx.doi.org/10.1016/j.conengprac.2016.03.010

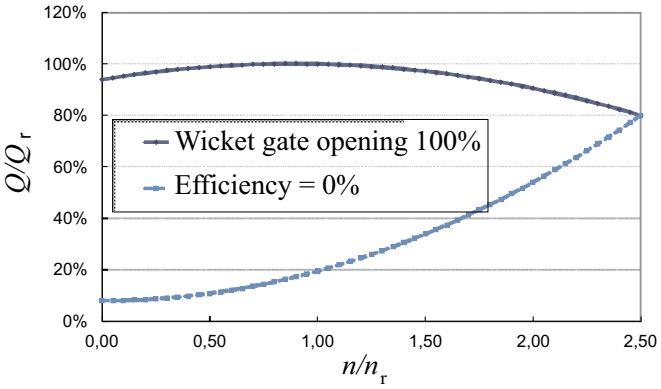

Fig. 2. Non-dimensional water flow rate Q/Q_r *vs.* non-dimensional rotational speed n/n_r.

The turbine curve at $G = 100\%$ (*i.e.* fully open wicked gate) is reported in Fig. 2, together with the curve at $\eta = 0\%$, so that the operating region allowed for the Francis turbine is defined. The water flow rate Q is calculated by means of (11) for any operating point, as a function of the current rotational speed n and wicked gate opening G.

The turbine torque M in (12) is a function of the water flow rate Q, the water level H and the rotational speed n. According to the relation (11), the turbine torque M is a function of the water level H, the rotational speed n and the wicked gate opening G:

$$\frac{M}{M_r} = \frac{\dfrac{Q}{Q_r}\dfrac{H}{H_r}}{\dfrac{n}{n_r}} = f_2(H, n, G) \tag{12}$$

Finally, the relations (13)–(16) express all the non-dimensional parameters for the turbine in terms of the corresponding relative deviations. Note that the definition of (16) allows only negative values for y:

$$\frac{Q}{Q_r} = 1 + q_t \tag{13}$$

$$\frac{H}{H_r} = 1 + h_t \tag{14}$$

$$\frac{n}{n_r} = 1 + x \tag{15}$$

$$G = 1 + y \tag{16}$$

where q_t represents the turbine flow rate relative deviation, h_t the turbine water pressure relative deviation, x the turbine speed relative deviation, and y the wicket gate servomotor stroke relative deviation.

If the generator unit supplies an isolated load, then the dynamic process of the generator unit considering the load characteristic can be represented as:

$$\frac{x}{m_t - m_{g0}} = \frac{1}{T_a\, s + e_g} \tag{17}$$

where m_{g0} is the load torque, T_a the generator unit mechanical time, and e_g the load self-regulation factor.

The Hydrodynamics System (HS) of Fig. 3 contains the tunnels, the penstock, and surge tanks, whilst Fig. 4 depicts the complete model. The turbine generator and the network of Fig. 4 represent

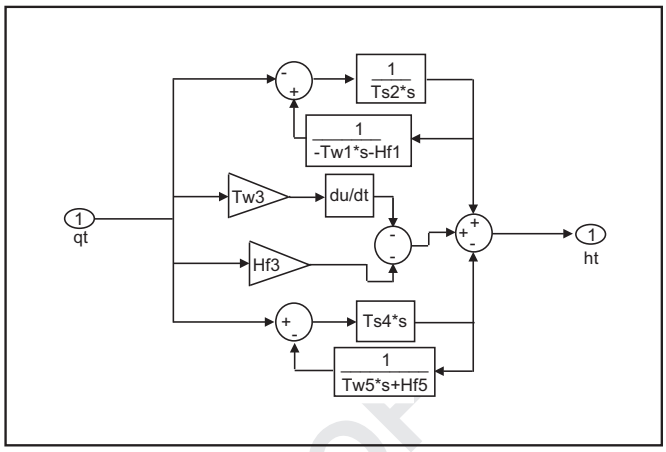

Fig. 3. Simulink block scheme of the Hydraulic System (HS).

the generator unit operating in isolation. Note that the du/dt block in Fig. 3 represents the derivative function of the Simulink software, which performs the numerical derivative with respect to the time of its input signal denoted as u.

A standard PID controller was applied to this power plant as described in Fang et al. (2008) to control the hydraulic turbine speed. Therefore, the control signal u is a function of the three PID parameters, K_p, K_i, and K_d, and depending on the turbine speed deviation x. Section 4 will analyse and compare the performance of this classic PID regulator designed in Fang et al. (2008) with respect to the adaptive and fuzzy control strategies proposed in this paper, and described in Section 3.

2.2. Hydraulic system fault modes

Regarding the fault cases analysed in this paper, it is assumed that they affect:

1. the servomechanism of the process (the actuator of the hydraulic turbine controller, *i.e.* an actuator fault), f_y;
2. the hydraulic turbine (the turbine flow rate, *i.e.* a system fault), f_q;
3. the hydraulic turbine speed sensor (*i.e.* a sensor fault), f_x.

Regarding the actuator fault f_y, if it is assumed that there is no further actuator dynamics in the current servomechanism, by neglecting smaller time constants, the analysed actuator fault f_y produces a slower response on the demanded wicket gate opening. It is also considered that the time constant of the actuator response increases linearly with time in order to represent an incipient (progressive) damage of the electric positioning motor. Only this actuator fault was preliminarily analysed in Simani et al. (2015).

The rationale of this fault derives from the consideration that many hydroelectric systems have servomotors that are operated by electric positioning motors. The actuator may be sluggish since the electric motor may slowly wear out over time, causing it to operate more slowly than normal. This problem could be caused by electrical faults, since, for example, internal windings may have begun to fail, or the motor may be binding internally. Moreover, mechanical ageing can mean bearing rust or a swelled rotor.

After these considerations, as described by the dashed line blocks in Fig. 4, the relationship between the control signal u and the wicket gate servomotor stroke y is thus expressed by means of a first-order model:

UNCORRECTED PROOF

Please cite this article as: Simani, S., et al. Fault tolerant control of a simulated hydroelectric system. *Control Engineering Practice* (2016), http://dx.doi.org/10.1016/j.conengprac.2016.03.010

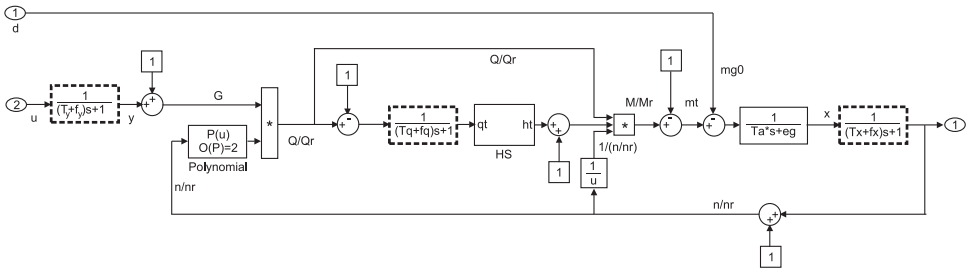

Fig. 4. Simulink layout of the hydraulic turbine, the generator unit and the network.

$$y = \frac{u}{(T_y + f_y)\, s + 1} \tag{18}$$

where $T_y + f_y$ is the wicket gate servomotor response time that increases with time, as it will be simulated in Section 4. The considered actuator fault f_y is modelled by means of a ramp function, since it represents the case of a slowly developing fault, which can be quite hard to detect, as already considered *e.g.* in Patton, Simani, Daley, and Pike (2000).

Two more fault cases are considered in this paper, which were not addressed in Simani et al. (2015). In particular, concerning the hydraulic turbine fault f_q, it is assumed that it modifies its flow rate, as shown in Fig. 4. Therefore, the turbine flow rate relation in Simani et al. (2015) is modified as:

$$q_t = \frac{1}{(T_q + f_q)\, s + 1}\left(\frac{Q}{Q_r} - 1\right) \tag{19}$$

in order to take into account the system fault effect. This results in a delayed variation of the turbine flow rate. The fault f_q is modelled as a gradual reduction in turbine flow rate over time, *i.e.* by means of a ramp function. Also the maximum decrease in turbine flow rate is set nominally at 5%, while the fault development rate is set to 5% reduction of the rated flow rate per hour, similar to the scenario addressed in Patton, Simani, et al. (2000).

Finally, the sensor fault f_x affects the measurement of the hydraulic turbine speed, as described in Fig. 4 with the modified relation in the form:

$$\frac{x}{(T_x + f_x)\, s + 1} = \frac{n}{n_r} - 1 \tag{20}$$

The fault f_x represents the malfunctioning of the speed sensor of the hydraulic turbine, which leads to a slowly increasing or decreasing reading over time. The fault development rate is set to 5% error in measuring actual speed per hour. Therefore, the fault f_x is modelled again as a ramp function, since it represents the case of a slowly developing malfunction. The fault f_x can also describe a delay in the hydraulic speed measurement, which is implemented with a positive or negative step function of appropriate amplitude.

It is worth observing that the model of the hydraulic system as well as the scenario of developing incipient faults adopted in this work takes into account the basic dynamic phenomena, and can be quite easily used for describing the realistic behaviour of general hydraulic processes (Fang et al., 2008; Kishor et al., 2007; Simani, Alvisi, et al., 2014; Simani et al., 2015).

Note finally that, in realistic applications, it is commonplace for the considered faults to develop slowly over a period of months or years. However, for the purpose of this paper, in order to avoid excessively long duration simulations, the faults development rate has been increased, so that significant effects are present after a few seconds. This factor must be taken into account in the FTC algorithm designs. The rate of development and magnitude of the faults have been set to typical values. In fact, one is usually interested to know how large the fault parameter can be made while still maintaining good performance. This represents one of the key issues of the paper, *i.e.* the viable application of practical FTC solutions to hydroelectric plants, which will be analysed in Section 4.

3. FTC scheme design strategies

This section briefly recalls the approaches exploited for obtaining the FTC strategies applied to the considered hydraulic system. In particular, the fuzzy modelling and identification scheme that enhances the design procedure of the proposed fuzzy FTC is briefly summarised in the following, without providing many details, since it was already addressed in Simani and Castaldi (2013) even if *without any fault tolerance features*. Moreover, the development of the adaptive control strategy proposed in connection with the on-line estimation scheme was already addressed in Simani, Alvisi, et al. (2014), but again without considering any fault tolerance properties.

In more detail, the Fuzzy Modelling and IDentification (FMID) scheme consists of two steps. First, the operating conditions are defined via a data clustering technique, in particular relying on the Gustafson–Kessel (GK) fuzzy clustering method, already available in Babuška (1998). The second step derives the FTC scheme, which is based on the identification of the FDD module for the fault reconstruction, and the derivation of the fuzzy controller for the fault compensation. This point is achieved using the identification procedure proposed in Simani, Fantuzzi, Rovatti, and Beghelli (1999). The TS fuzzy models finally derived here have the general form of:

$$y(k+1) = \frac{\sum_{i=1}^{M} \mu_i\Big(\mathbf{x}(k)\Big)\, y_i}{\sum_{i=1}^{M} \mu_i\Big(\mathbf{x}(k)\Big)} \tag{21}$$

where $y_i = \mathbf{a}_i\, \mathbf{x} + b_i$, with $\mathbf{a}_i$ being the parameter vector (regressand), and b_i the scalar offset. M is the number of clusters. $\mathbf{x} = \mathbf{x}(k)$ represents the regressor vector, which can contain delayed samples of $u(k)$ and $y(k)$. The *antecedent* fuzzy sets μ_i are extracted from the fuzzy partition matrix (Babuška, 1998). The *consequent parameters* $\mathbf{a}_i$ and b_i are estimated from the data using the procedure presented *e.g.* in Simani et al. (1999).

It is worth noting that the fuzzy identification approach is proposed here as it is able to approximate any nonlinear functions. In this way, both the FDD (for fault estimation) and the fuzzy controller (for fault compensation) modules, which compose the FTC fuzzy scheme, are directly identified by exploiting the suggested FMID strategy.

In fact, if the continuous-time behaviour of the hydraulic system is described as the model (21), its TS fuzzy prototype has the specific form:

UNCORRECTED PROOF

Please cite this article as: Simani, S., et al. Fault tolerant control of a simulated hydroelectric system. *Control Engineering Practice* (2016), http://dx.doi.org/10.1016/j.conengprac.2016.03.010

$$y(k+1)=\frac{\sum_{i=1}^{M}\mu_i^{(m)}\left(\mathbf{x}^{(m)}(k)\right)\left(\mathbf{a}_i^{(m)}\,\mathbf{x}^{(m)}(k)+b_i^{(m)}\right)}{\sum_{i=1}^{M}\mu_i^{(m)}\left(\mathbf{x}^{(m)}(k)\right)} \tag{22}$$

The input of the model is the current state $\mathbf{x}^{(m)}(k)$ that collects the lagged inputs $u(k)$ and outputs $y(k)$, as well as the input $f(k)$. The output is a prediction of the hydroelectric process output at the next sample $y(k+1)$. In (22) the estimated membership functions $\mu_i^{(m)}$, the state $\mathbf{x}^{(m)}$, and the parameters $\mathbf{a}_i^{(m)}$, $b_i^{(m)}$ of the monitored system are denoted by the superscript (m).

Once the fuzzy description of the system under diagnosis has been achieved, the next step is the derivation of the FDD module. As already remarked, the objective of the FDD fuzzy model is to reconstruct the input $\hat{f}(k)$, *i.e.* the fault function. When this signal is injected into the FTC system, the process output at $k+1$ has to be equal to the desired output $y(k+1)$, even in the presence of faults. In principle, this could be obtained by inverting the plant model under diagnosis.

In general, the fault $\hat{f}(k+1)$ results to depend on the plant state $\mathbf{x}^{(m)}(k)$ and its output $y(k)$. In this way, the fault function is described again as a model in the form of (21), which is represented as the following equation:

$$\hat{f}(k+1)=\frac{\sum_{i=1}^{M}\mu_i^{(e)}\left(\mathbf{x}^{(e)}(k)\right)\left(\mathbf{a}_i^{(e)}\,\mathbf{x}^{(e)}(k)+b_i^{(e)}\right)}{\sum_{i=1}^{M}\mu_i^{(e)}\left(\mathbf{x}^{(e)}(k)\right)} \tag{23}$$

where the input signals feeding the estimated FDD module are the state $\mathbf{x}^{(e)}(k)$, which depends on the system model state $\mathbf{x}^{(m)}(k)$, and the plant output $y(k)$.

Note that, as described in Babuška (1998), both the controller and process model states contain the lagged input and output signals. For the case of the fuzzy controller model, its state $\mathbf{x}^{(e)}(k)$ contains the same lagged inputs and the outputs of the fuzzy model of the process, *i.e.* the state $\mathbf{x}^{(m)}(k)$. However, $\mathbf{x}^{(e)}(k)$ also includes the reference signal. It is worth noting that this scheme resembles the MRAC exploited in the Matlab/Simulink tool for estimating the neural network controller from the input–output data of the closed-loop controller process. Moreover, this scheme prevents the closed-loop scheme from possible instability during the identification stage.

In (23), the estimated membership functions $\mu_i^{(e)}$ and the parameters $\mathbf{a}_i^{(e)}$, $b_i^{(e)}$ are denoted with the superscript (e), as they represent the parameters of the fault reconstructor. The derivation of the model in the form of (23) follows again the procedure described in Simani and Castaldi (2013). In particular, the data acquired from the process operating regions already defined using the GK algorithm are exploited again for the derivation of the parameters $\mu_i^{(e)}$, $\mathbf{a}_i^{(e)}$ and $b_i^{(e)}$.

Note that, Simani, Farsoni, and Castaldi (2014), in the case of a simulated wind turbine benchmark, showed that the fault reconstructor (23) is able to predict any fault functions with arbitrary accuracy, which depends on uncertainty and disturbance levels.

Once derived the FDD module and with the fault estimation $\hat{f}(k)$, it is possible to develop the FTC model. This FTC module generates the control input $u(k)$ that feeds the monitored process, thus allowing to achieve the required fault tolerance capabilities. The FTC model is described again by a fuzzy TS model again in the form (21). It depends on the process model state $\mathbf{x}^{(m)}(k)$, the reconstructed fault $\hat{f}(k)$ (23), and the actual process output $y(k)$.

Therefore, the series connection of the FTC block with the plant leads to an identity mapping, when the signal $\hat{f}(k)$ generated by the FDD block is such that $y(k+1)=F(\mathbf{x}(k),\hat{f}(k))$. It is worth noting that the control input $\hat{u}(k)$ provided by the FTC module feeds the process model and depends on the plant state $\mathbf{x}^{(m)}(k)$. However, due to modelling errors and disturbance, the fuzzy estimation task is able to make the difference between the controlled and the desired outputs arbitrarily small by an appropriate choice of the tuning parameters of the fuzzy models, *i.e.* the number of clusters M. In fact, as addressed in Simani et al. (1999), the optimal number of cluster M is defined by optimising a performance function $J(M)$ that takes into account both the tracking error and the model approximation properties. The same remarks are valid for the parameters of the FTC fuzzy module. The fuzzy model of the process is exploited for the recursive prediction of the state vector $\mathbf{x}(k)$, *i.e.* $\mathbf{x}^{(m)}(k)$. Further details are provided in Simani et al. (1999). In this way, the states of the fuzzy FDD and FTC models are updated using the state of the estimated process model $\mathbf{x}^{(m)}(k)$, the reconstructed control input $\hat{u}(k)$ and the monitored output $y(k)$. Apart from the computation of the membership degrees $\mu_i^{(m)}$, the parameters of the fuzzy models are derived using standard matrix operations and linear interpolations, thus making the methodology suitable also for real-time realisations.

The fault reconstruction $\hat{f}(k)$ from the FDD module (23) is thus used for the compensation of the control signal $\hat{u}(k)$ generated by the FTC block and injected into the hydroelectric plant. The FTC block is fed by the reconstructed fault $\hat{f}(k)$ from the FDD module. After this correction, the FTC scheme provides the correct tracking of the set-point signal. The complete AFTCS relying on the fuzzy FDD and FTC blocks is represented in Fig. 5 .

Fig. 5 represents the FTC module output $\hat{u}$, *i.e.* the wicket gate servomotor stroke, and y is the hydroelectric process output. $\hat{f}$ is the fault affecting the hydraulic process, whilst x is the hydroelectric process output, *i.e.* the turbine speed relative deviation. The Analog-to-Digital (A/D) and Digital-to-Analog (D/A) converters are also sketched. Therefore, Fig. 5 highlights how the complete AFTCS is achieved by integrating the identified fuzzy FDD module with the estimated FTC block. The FDD module generates the estimate of the fault signal $\hat{f}$, which is injected into the FTC module, in order to compensate the effect of the actuator fault, and for generating the control signal $\hat{u}$.

It is worth highlighting the strategy applied in this paper for achieving the required fault tolerance characteristics. With reference to the controller identification, its parameters are estimated by means of the same algorithm applied for identifying the fuzzy models, and by considering the *faulty sequences*. Therefore, the optimal controller performances with respect to set-point variations are validated and enhanced for the faulty working conditions. In this way, if both the fuzzy model identification and the fault reconstructor estimation are properly performed, the scheme of Fig. 5 leads to good fault tolerance properties, as demonstrated in Simani and Castaldi (2013). Moreover, in general, the proposed fuzzy solution works for the fault cases that are considered at the design phase. If different fault scenarios are

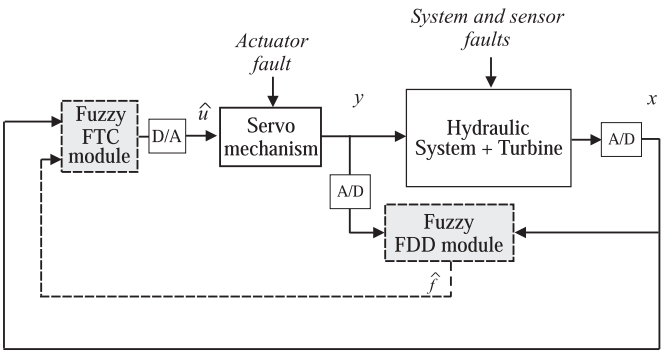

Fig. 5. Diagram of the AFTCS based on the FMID strategy.

UNCORRECTED Proof

Please cite this article as: Simani, S., et al. Fault tolerant control of a simulated hydroelectric system. *Control Engineering Practice* (2016), http://dx.doi.org/10.1016/j.conengprac.2016.03.010

considered, this situation might require a new fuzzy identification procedure.

The remainder of this section recalls the methodology used for obtaining the Linear Parameter Varying (LPV) description of the hydraulic process, which is exploited for the development of the adaptive control strategy. In particular, the on-line estimation scheme exploiting the Least Mean Squares (LMS) with adaptive directional forgetting proposed in this work enhances the design procedure of the suggested adaptive FTC scheme. Note that this approach can be seen as a PFTCS. This strategy, which is an improvement with respect to classical LMS (Ljung, 1999) and LMS with exponential forgetting (Kulhavý, 1987), was already considered in Simani, Alvisi, et al. (2014) but without any fault tolerance properties. A different adaptive strategy was presented in Simani and Castaldi (2013) and applied to a wind turbine benchmark.

Briefly, the LSM with adaptive directional forgetting provides the on-line estimation of a LPV model of the hydraulic system, *i.e.* identified model parameters computed at each time step k. This on-line estimation procedure was implemented in the Matlab® and Simulink® environments, as described in Bobal et al. (2005). Once the LPV parameters of the model approximating the behaviour of the hydraulic process have been computed at each time step k, the adaptive PI controller is obtained, for example exploiting the Ziegler–Nichols adaptive methodology addressed in Bobal et al. (2005), and proposed in Simani, Alvisi, et al. (2014) but without fault tolerance capabilities.

The proposed PFTCS relying on the adaptive PI regulator is used for the control of the wicket gate servomotor stroke y. The implementation scheme is sketched in Fig. 6.

Fig. 6 highlights how the adaptive controller should be able to cope with any possible faulty situations. In this case, the adaptive controller uses the hydraulic process output x, namely the hydraulic turbine speed, whilst the actuated control input is y.

Also in this case, it is worth highlighting the strategy applied for achieving the required active fault tolerance characteristics. With reference to the adaptive control scheme of Fig. 6, the parameters are estimated by considering the *faulty data sequences*. Therefore, the optimal controller performances with respect to set-point variations are enhanced also for the faulty working conditions. In this way, if both the model on-line identification and on-line estimation methods are properly performed, the parameter adaptation mechanisms will lead to acceptable active fault tolerance properties. Also, the motivation of using the proposed approach compared to other efficient FTC techniques is eluded.

Note finally that Fig. 6 shows only the diagram of the AFTCS that relies on adaptive control and on-line estimation strategies. In case the servomechanism does not receive any control signals due to disconnections, a supervisory system may be also added to guarantee plant safe working conditions, even in case of unscheduled shutdown.

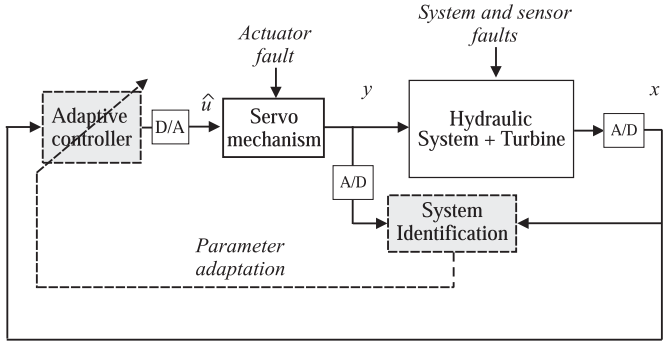

Fig. 6. Diagram of the PFTCS relying on adaptive control and on-line estimation method.

4. Simulation results

The hydraulic model recalled in Section 2 and the Francis turbine addressed in Simani, Alvisi, et al. (2014) were tuned in order to obtain the behaviour of the hydraulic process described in Fang et al. (2008). The main parameters of the hydraulic system are the following:

- Reservoir water level H_r: 400 m.
- Water flow rate Q_r: 36.13 m^3/s.
- Turbine power P_r: 127.6 MW.
- Turbine rotational speed n_r: 500 rpm.
- Turbine efficiency η_r: 90%;
- Turbine-rated torque: 2437 kN m;

The discrete-time data sequences x and y used for identification purpose were acquired with a sampling rate of 0.1 s from the hydraulic system.

Concerning the fuzzy scheme sketched in Section 3, the GK algorithm with $M=4$ clusters and a number of shifts $n=3$ were exploited for estimating the TS fuzzy description of the hydraulic system using the fault-free sampled data x and y. Therefore, the output x of the hydroelectric system described in Section 2 is approximated by a TS fuzzy Single-Input Single-Output (SISO) model in the form of (21). Using this TS fuzzy model, the estimation approach recalled in Section 3 was exploited again for identifying both the FDD and FTC modules of Fig. 5. According to Section 3, the parameters of the fuzzy FDD and FTC models were obtained by considering a number of clusters $M=4$ and fourth order ($n=4$) TS fuzzy prototypes.

It is worth noting the strategy used for obtaining the required fault tolerance characteristics. With respect to the FDD and FTC modules, the parameters of these fuzzy TS prototypes were obtained by considering the *faulty* sequences. In this way, the optimal FTC behaviour with respect to set-point variations were optimised for the *faulty* conditions of the process. Therefore, if the identification of process model followed by the FDD and FTC fuzzy estimation are properly performed, acceptable fault tolerance capabilities are obtained. Moreover, if the estimation of the FDD module has been correctly performed, this FDD block should be able to provide the correct reconstruction of any faulty conditions, even if they are different for the ones addressed in Section 2. In this way, this approach represents an AFTCS.

Concerning the adaptive approach sketched in Section 3, the hydraulic system is approximated via a LPV SISO (discrete-time) second order model. It is worth noting that the on-line estimation procedure recalled in Section 3 was performed using two different data sets. The first sequence consists of the fault-free data, whilst the second one contains the faulty data. Therefore, the LPV model parameters are identified in order to minimise the model-reality mismatch, *i.e.* the difference between the fault-free and the fault behaviour of the hydraulic process. In this way, the on-line estimated LPV prototype should lead to the optimal fitting of both the fault-free and the faulty working situations. Using this identified LPV prototype, the model-based approach for deriving the adaptive controller parameters is exploited and applied to the hydraulic benchmark. Thus, according to Simani, Alvisi, et al. (2014), the parameters of the adaptive PI controller were computed. In particular, the adaptive controller initialisation parameters were set to $\Theta_0 = [0.1,\ 0.2,\ 0.3,\ 0.4]^T$, $C_0 = 10^9\, I_4$, $\varphi_0 = 1$, $\lambda_0 = 0.001$, $\rho = 0.99$, and $\nu_0 = 10^{-6}$. The steady-state values of these parameters after the adaptation phase, due to the simulated faults and working conditions, are shown in Table 1.

Also in this case it is worth remarking the achieved fault tolerance features that are obtained with this *adaptive* strategy. The parameters of the PI adaptive controller have been derived using

UNCORRECTED PROOF

Please cite this article as: Simani, S., et al. Fault tolerant control of a simulated hydroelectric system. *Control Engineering Practice* (2016), http://dx.doi.org/10.1016/j.conengprac.2016.03.010

Table 1
Steady-state values of the LPV models.

Fault case	Torque value m_{g0} (%)	Final value Θ_0 MPS-NO-SPC
f_y	+100	$[-1.7466, -1.1411, 0.8605, 1.1411]^T$
	−100	$[-1.4533, 4.4571, 0.0002, -4.4477]^T$
f_q	+100	$[-1.7095, -1.3063, 0.8422, 1.3063]^T$
	−100	$[-2.0118, 0.5375, 0.9537, -0.5375]^T$
f_x	+100	$[-1.8606, -0.6181, 0.9228, 0.6180]^T$
	−100	$[-1.0196, -0.0360, 0.2572, 0.0377]^T$

the Ziegler–Nichols rules, applied to the LPV model and considering the faulty sequences. Therefore, the optimal controller behaviour is maximised with respect to set-point variations also for the *faulty* situations. In this way, if both the on-line parametric identification and the tuning procedure of the PI adaptive regulator are properly performed, the parameter adaptation mechanisms can lead to acceptable passive fault tolerance properties. In fact, the estimation of the LPV model is achieved using the faulty data of the hydraulic process. However, by means of the proposed adaptation mechanism, the proposed adaptive FTC scheme could not be able to maintain good control performances when fault conditions different for the ones summarised in Section 2 are simulated. Therefore, this strategy belongs to the PFTCS family.

In the following, the suggested fuzzy and adaptive FTC solutions, and the classical control strategy addressed in Fang et al. (2008) have been applied and compared in the Matlab® and Simulink® environments. In particular, the PID parameters described in Fang et al. (2008) were $K_d=1$ for the derivative gain, $K_i=0.2$ for the integral term, and $K_p=1$ for the proportional gain.

The efficacy of the controllers presented in Section 3 have been assessed in simulation by considering different load torque m_{g0} variations described by step and ramp functions, as reported in Simani, Alvisi, et al. (2014). The fault cases f_y, f_q and f_x considered in the relations (18), (19) and (20) recalled in Section 2 are depicted in Fig. 7.

In particular, the fault signals f_y, f_q and f_x are thus modelled by means of the ramp function depicted in Fig. 7. As remarked in Section 2, these situations represent incipient faults, which are hard to detect. Moreover, Fig. 7 shows that the development rate of these faults has been imposed equal to 5%. These incipient fault modes were already considered for the case of a gas turbine, as addressed in Patton, Simani, et al. (2000). According to Fig. 7, the injected fault commences at 0 s. Only the fault f_x was also described as an abrupt change of the hydraulic turbine speed sensor reading, thus representing a delay in the signal from the measurement sensor x, which is 0.06 s.

This paper also considers the case of the simultaneous occurrence of the three previous faults, as well as the complete drop of the rotational speed sensor.

As an example, with reference to the fault f_y, the results summarised in Fig. 8 over 60 s highlight that, even though the three regulators can maintain the relative deviation of the rotational speed zero (*i.e.* the rotational speed constant) in steady-state conditions, the FTC performances of both the fuzzy and adaptive controllers in faulty conditions are better than those of the classic PID governor developed in Fang et al. (2008).

The same results are achieved by considering more severe situations corresponding to load torque m_{g0} changes in start-up and shutdown conditions over 900 s. In this case, Fig. 9 depicts that the relative deviation of the rotational speed is maintained at zero in steady-state conditions. Moreover, the capabilities of the fuzzy FTC strategy are better than those of the remaining governors.

With reference to the fault f_y accommodation, an example of

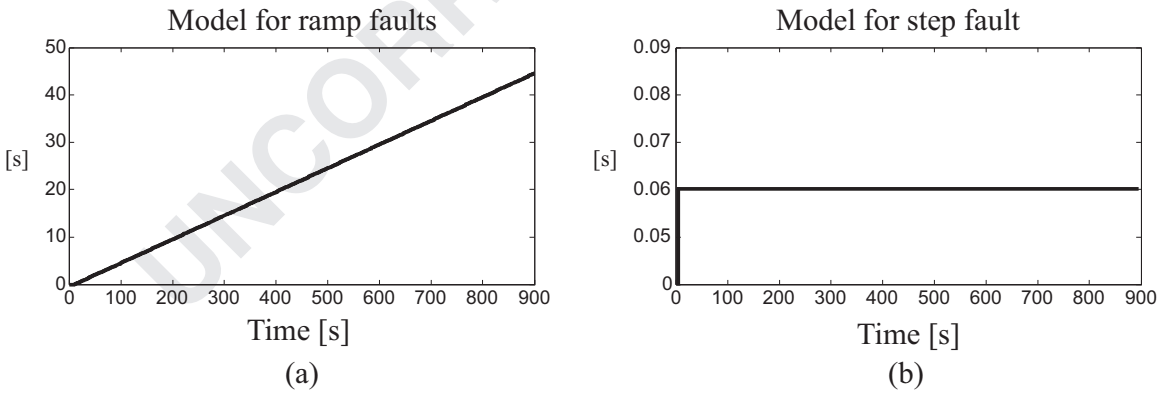

Fig. 7. Models for (a) the ramp fault affecting the wicket gate actuator (f_y), the hydraulic turbine (f_q) and its speed measurement sensor (f_x), and (b) the step fault affecting the speed measurement sensor (f_x).

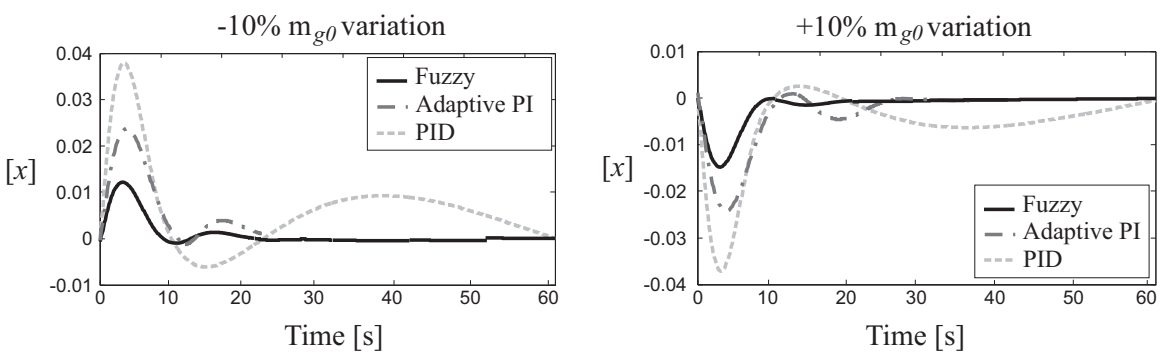

Fig. 8. Fault f_y: turbine speed relative deviations x when the load torque m_{g0} changes by ±10%.

UNCORRECTED PROOF

Please cite this article as: Simani, S., et al. Fault tolerant control of a simulated hydroelectric system. *Control Engineering Practice* (2016), http://dx.doi.org/10.1016/j.conengprac.2016.03.010

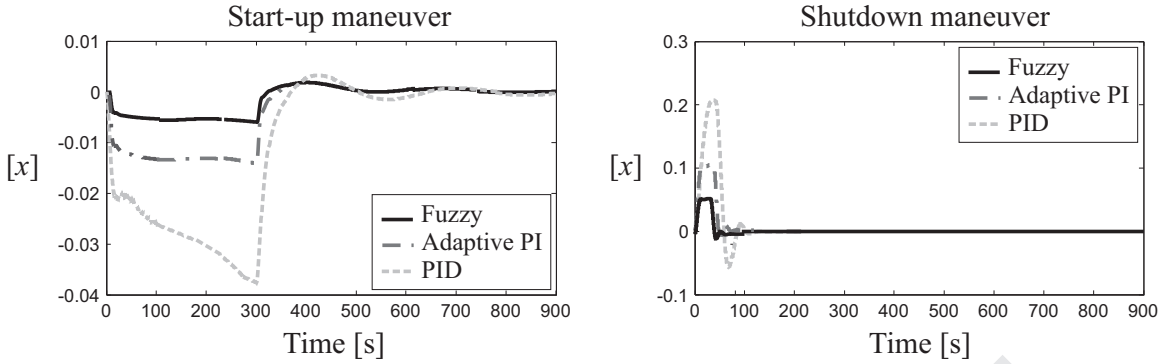

Fig. 9. Fault f_y: turbine speed relative deviations x when the load torque m_{g0} changes during start-up and shutdown.

the structure of the FTC fuzzy controller is reported in the form of (24), as sketched in Fig. 5.

$$
\begin{aligned}
\text{Rule 1: } u(k) &= 0.02\,x(k) + 0.97\,x(k-1) - 0.89\,x(k-2) + 0.41\,x(k-3) \\
&\quad + 0.09\,x(k-4) + 0.24\,\hat{f}_y(k-1) - 0.121\,\hat{f}_y(k-2) \\
&\quad + 0.34\,\hat{f}_y(k-3) - 0.21\,\hat{f}_y(k-4) - 0.37\,u(k-1) \\
&\quad - 0.61\,u(k-2) + 0.47\,u(k-3) + 0.21\,u_5(k-4) + 0.16 \\
\text{Rule 2: } u(k) &= 0.07\,x(k) + 1.04\,x(k-1) - 0.31\,x(k-2) - 0.12\,x(k-3) \\
&\quad - 0.23\,x(k-4) + 0.32\,\hat{f}_y(k-1) - 0.17\,\hat{f}_(k-2) - 0.11\,\hat{f}_(k \\
&\quad - 3) - 0.22\,\hat{f}_y(k-4) - 0.62\,u(k-1) + 0.12\,u(k-2) \\
&\quad + 0.54\,u_3(k-3) - 0.16\,u(k-4) + 0.1 \\
\text{Rule 3: } u(k) &= 0.13\,x(k) - 0.94\,x(k-1) + 0.37\,x(k-2) + 0.18\,x(k-3) \\
&\quad - 0.10\,x(k-4) + 0.06\hat{f}_y(k-1) + 0.84\,\hat{f}_y(k-2) \\
&\quad - 0.26\,\hat{f}_y(k-3) + 0.18\,\hat{f}_y(k-4) + 0.27\,u(k-1) \\
&\quad + 0.85\,u(k-2) - 0.34\,u(k-3) + 9.10\cdot10^{-2}\,u(k-4) \\
&\quad + 1.72\cdot10^{-2} \\
\text{Rule 4: } u(k) &= -0.37\,x(k) + 0.83\,x(k-1) + 3.01\cdot10^{-2}\,x(k-2) \\
&\quad + 0.11\,x(k-3) + 0.27\,x(k-4) - 0.05\,\hat{f}_y(k-1) \\
&\quad + 0.19\,\hat{f}_y(k-2) + 0.03\,\hat{f}_y(k-3) - 1.56\cdot10^{-2}\,\hat{f}_y(k-4) \\
&\quad + 1.75\,u(k-1) + 0.35\,u(k-2) - 0.23\,u(k-3) \\
&\quad - 0.27\,u(k-4) - 0.02
\end{aligned}
\tag{24}
$$

The expression (24) shows that this fuzzy controller uses the signals $x(k)$ and $\hat{f}_y(k)$ on the basis of the identified consequents for each rule, with $M = 4$ rules and order $n = 4$. Moreover, its identified membership functions for x are depicted in Fig. 10.

Concerning the LPV models, the adaptive controller parameters from their initial conditions reach their steady-state values summarised in Table 1. Their values are different due to the simulated faults and the working conditions of the system. The variations of the adaptation law variables φ_0, λ_0, ρ, C_0 and ν_0 are not reported here.

Regarding the fault f_q, the simulation results are summarised in Fig. 11, which shows the achievement of the required FTC properties in both transient and steady-state conditions.

Even for the more severe start-up and shutdown conditions over 900 s, Fig. 12 shows that the relative deviation of the rotational speed is maintained to zero in steady-state. Moreover, the performance of the fuzzy FTC strategy is better than those of the remaining governors.

The simulation results concerning the fault f_x are summarised in Fig. 13. Also in this case, the required FTC properties are achieved for both the fuzzy and PI adaptive controllers.

Again, the features of the designed fault tolerant controllers are maintained by considering the load torque m_{g0} changes in start-up and shutdown conditions, as shown in Fig. 14. Note that different simulation times are used in order to highlight the transient behaviour. Also in this case, the performance of the fuzzy FTC strategy results preferable with respect to those achievable by means of the remaining governors.

Fig. 15 reports the results of the simultaneous occurrence of the faults f_y, f_q, and f_x by considering the load torque m_{g0} changes during start-up and shutdown. Again, also for this severe situation, the features of the fuzzy FTC strategy are better than the ones obtained with the remaining governors.

Fig. 16 shows the case of the complete drop of the rotational speed sensor for the most severe conditions over 900 s. In this condition, the fuzzy FTC scheme is able to maintain the control of the relative deviation of the rotational speed. In fact, only in this case, the FDD block of Fig. 5 is able to compensate for the complete loss of the measured variable by means of the injected input $\hat{f}$, which is thus used as controller variable x. In this case the fuzzy FTC module uses the reconstruction of the signal f as a virtual (software) sensor of the turbine speed x, as the actual measurement is not available.

Table 2reports the percent Normalised Sum of Squared tracking Error (*NSSE%*) values that are computed for both the controllers and different data sequences.

Note that the previous simulations considered rate of development and magnitude of the faults set to typical values. However, one can be interested to know how large the fault parameters can be made in order to maintain good performance. These values are summarised in Table 3, which reports the fault rates for the most severe conditions over 900 s.

Some final comments are drawn here. For the proposed FTC solutions, the behaviour of the controlled system is always stable. On the other hand, the standard PID is not always able to guarantee a stable response also in faulty conditions. The *NSSE%* values for both the adaptive PI and the fuzzy solutions are smaller than

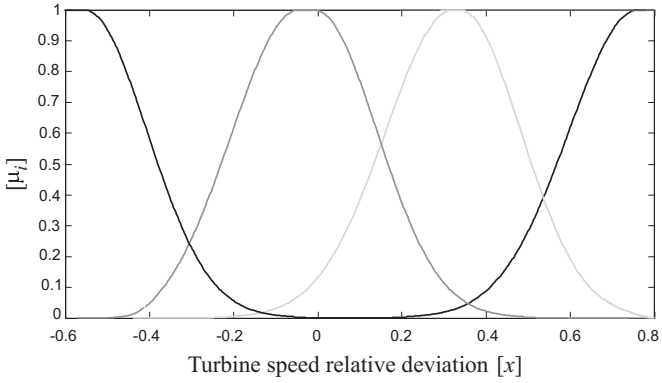

Fig. 10. Membership functions for x used by the FTC fuzzy controller for fault f_y accommodation.

UNCORRECTED PROOF

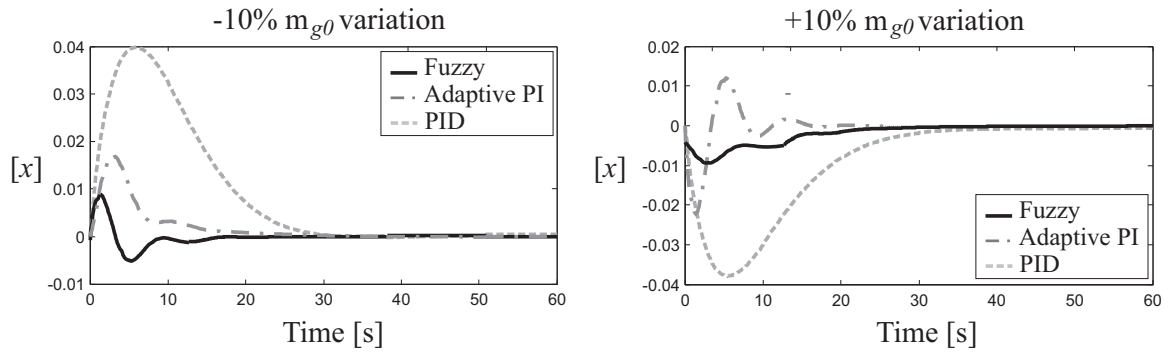

Fig. 11. Fault f_q: turbine speed relative deviations x when the load torque m_{g0} changes by ±10%.

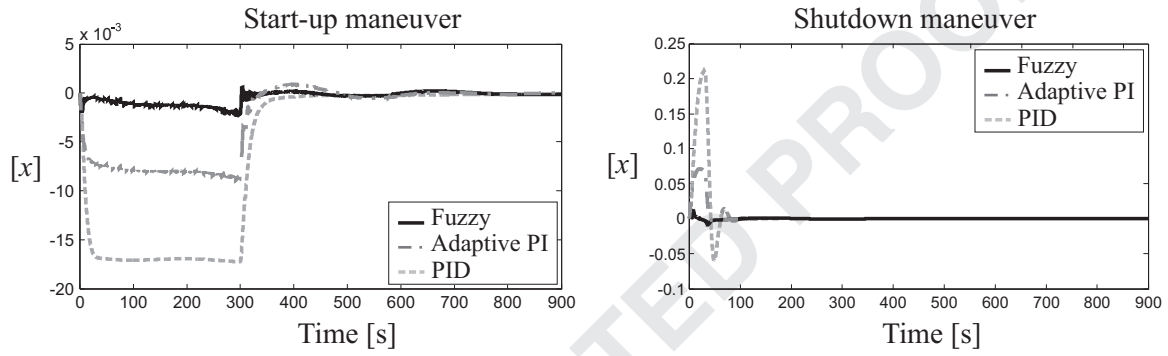

Fig. 12. Fault f_q: turbine speed relative deviations x when the load torque m_{g0} changes during start-up and shutdown.

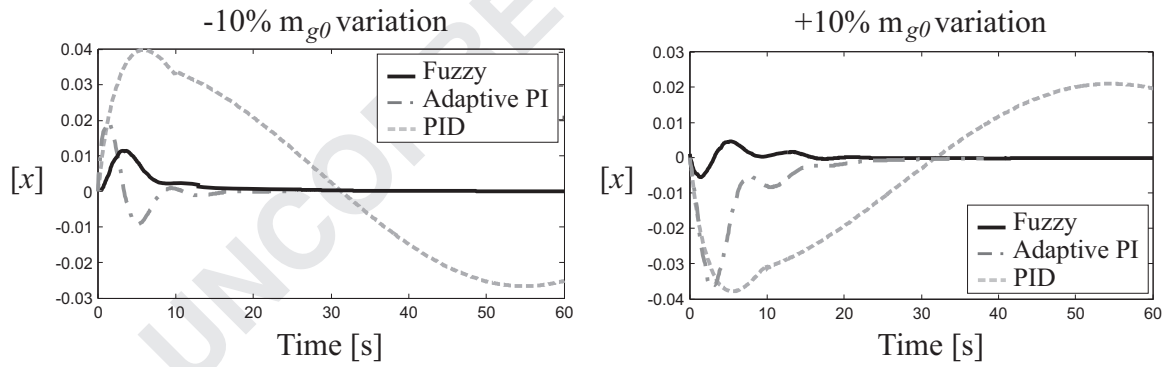

Fig. 13. Fault f_x: turbine speed relative deviations x when the load torque m_{g0} changes by ±10%.

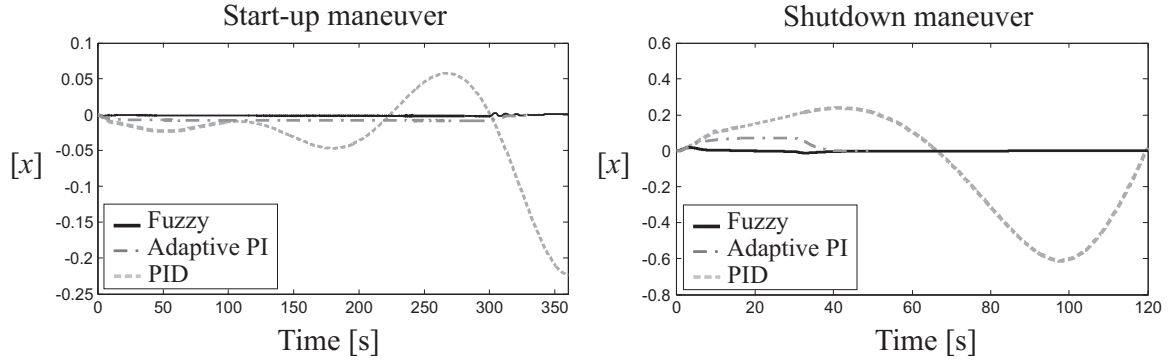

Fig. 14. Fault f_x: turbine speed relative deviations x when the load torque m_{g0} changes during start-up and shutdown.

UNCORRECTED PROOF

Please cite this article as: Simani, S., et al. Fault tolerant control of a simulated hydroelectric system. *Control Engineering Practice* (2016), http://dx.doi.org/10.1016/j.conengprac.2016.03.010

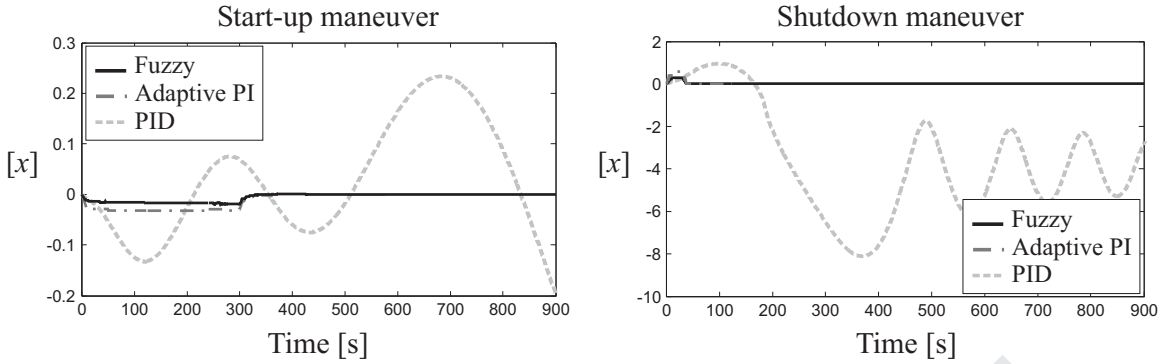

Fig. 15. Simultaneous faults f_y, f_q, and f_x: turbine speed relative deviations x when the load torque m_{g0} changes during start-up and shutdown.

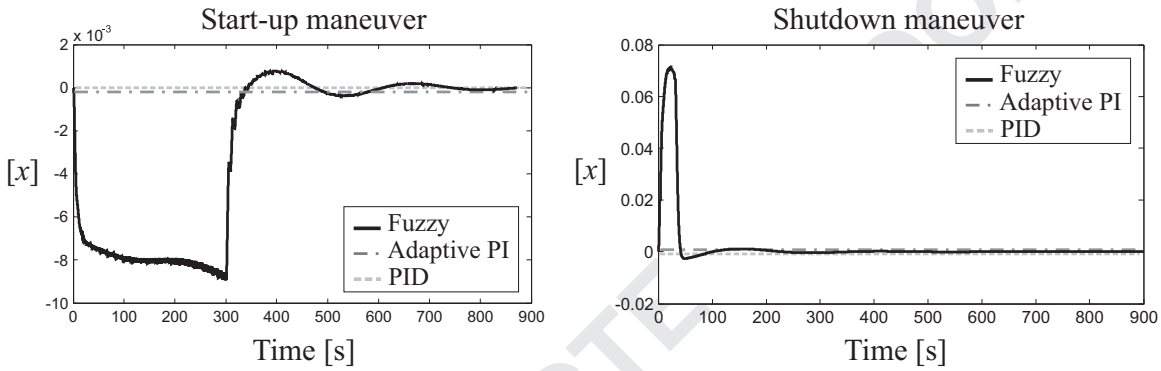

Fig. 16. Complete drop of the rotational speed sensor: turbine speed relative deviations x when the load torque m_{g0} changes during start-up and shutdown.

Table 2
Comparison of the capabilities of the controllers in faulty conditions with nominal parameters.

Fault case	Torque value m_{g0} (%)	Fuzzy *NSSE%*	Adaptive PI *NSSE%*	PID *NSSE%*
f_y	+1	0.01	0.06	0.14
	−1	0.01	0.05	0.13
	+10	0.16	0.60	1.34
	−10	0.12	0.59	1.38
	+100	0.08	0.63	6.17
	−100	0.38	3.07	Unstable
f_q	+1	0.01	0.06	0.13
	−1	0.01	0.05	0.12
	+10	0.16	0.60	1.24
	−10	0.12	0.59	1.29
	+100	0.08	0.62	1.32
	−100	0.44	3.07	10.27
f_x	+1	0.06	0.11	26.27
	−1	0.05	0.11	23.31
	+10	0.16	0.61	Unstable
	−10	0.11	0.57	Unstable
	+100	0.08	0.63	Unstable
	−100	0.43	3.79	Unstable
f_q, f_y, f_x	+100	0.65	3.78	Unstable
multiple faults	−100	2.35	8.45	Unstable
f_x sensor	+100	0.21	NA	NA
drop	−100	0.57	NA	NA

the ones achievable by the standard PID. Moreover, the fuzzy solution leads to *NSSE%* values smaller than the adaptive PI, especially for large variations of the load torque m_{g0}. These features derive from the adaptive behaviour of the PI, even if the fuzzy solution allows to achieve even better performance due to the explicit fault compensation of the FTC scheme.

Table 3
Maximum tolerated fault rate by using different FTC schemes.

Fault case	Torque value m_{g0} (%)	Fuzzy (%)	Adaptive PI (%)	PID (%)
f_y	+100	27	18	8 MPS-NO-SPC
	−100	17	11	3 MPS-NO-SPC
f_q	+100	45	17	7 MPS-NO-SPC
	−100	37	10	8 MPS-NO-SPC
f_x	+100	31	15	2 MPS-NO-SPC
	−100	28	11	1

4.1. Reliability and sensitivity analysis of the FTC solutions

In this section, extensive simulations are presented through the hydraulic system and a Monte-Carlo analysis. In this case, the Monte-Carlo tool is fundamental since the FTC performances depend on the model-reality mismatch, which is simulated in this work by means of suitable parameter variations.

In particular, the hydroelectric simulator in the Simulink® environment was also able to statistically change the parameters of the model in order to introduce possible parameter variations. Under this assumption, Table 4 summarises the nominal values of the hydraulic system variables (Fang et al., 2008; Simani, Alvisi, et al., 2014).

The Monte-Carlo analysis is thus proposed here for analysing the reliability and parameter sensitivity properties of the proposed FTC solutions. Therefore, the hydraulic system parameters have been modelled as Gaussian variables with standard deviations of ±20% with respect to their nominal values summarised in Table 4. The average values of the *NSSE%* index were computed and evaluated over 100 Monte-Carlo runs in faulty conditions.

UNCORRECTED PDF

Please cite this article as: Simani, S., et al. Fault tolerant control of a simulated hydroelectric system. *Control Engineering Practice* (2016), http://dx.doi.org/10.1016/j.conengprac.2016.03.010

Table 4
Nominal values of hydraulic system parameters varied by ±20% to perform the Monte-Carlo analysis.

Model variable	a	b	c	H_{f_1}	H_{f_3}	H_{f_5}	T_a	T_c	T_{s_2}	T_{s_4}	T_{w_1}	T_{w_3}	T_{w_5}
Nominal value	−0.08	0.14	0.94	0.0481 m	0.0481 m	0.0047 m	5.9 s	20 s	476.05 s	5000 s	3.22 s	0.83 s	0.1 s

Table 5
Monte-Carlo analysis for the designed controllers: *NSSE%* average values with parameter variations.

Fault case	Torque value m_{g0} (%)	Fuzzy *NSSE%*	Adaptive PI *NSSE%*	PID *NSSE%*
f_y	+1	0.02	0.07	0.14
	−1	0.02	0.07	0.14
	+10	0.25	0.70	1.43
	−10	0.19	0.67	1.44
	+100	1.01	1.21	6.25
	−100	0.41	3.20	Unstable
f_q	+1	0.02	0.07	0.14
	−1	0.02	0.07	0.13
	+10	0.26	0.71	1.31
	−10	0.19	0.68	1.37
	+100	1.10	1.18	1.35
	−100	0.50	3.96	10.59
f_x	+1	0.02	0.07	Unstable
	−1	0.02	0.07	Unstable
	+10	0.26	0.71	Unstable
	−10	0.19	0.67	Unstable
	+100	1.21	1.41	Unstable
	−100	0.49	3.87	Unstable

Table 5 summarises the values of the considered performance index *NSSE%*, with reference to all the possible combinations of the random parameters described in Table 4. Table 5 shows that the proposed control schemes, and in particular the fuzzy solution, allow to maintain good control performances even in the presence of considerable error and uncertainty, *i.e.* up to ±100% variation of the torque and up to ±20% of model parameter changes.

The results reported in Table 5 highlight that both the adaptive PI and the fuzzy controllers proposed in this paper (which have been both designed to be fault tolerant) allow to achieve better performance than the PID governor, especially for large variations of the load m_{g0}. Moreover, it can be observed that the robustness features of the fuzzy controller are better than those of the adaptive PI controller. It is worth noting also that the presented PFTCS (adaptive) and AFTCS (fuzzy) solutions allow to achieve the control objective recovery, the transient characteristics and the reference trajectory tracking when a fault is acting on the hydraulic system. However, the asymptotic fault accommodation, the transient and the asymptotic stability of the controlled process, which in this paper were assessed in simulation only, may require further investigations.

Some more general comments are drawn regarding the capability of the proposed FTC controllers. In general, the *NSSE* values are lower for reduced variations of the load torque and considerably lower in case of significant transient maneuvers (*i.e.* start-up and shutdown). Moreover, though always lower, in some cases the settling time is not significantly decreased and remains comparable to those obtainable by means of a standard PID. This is probably due to the inherent dynamics of the simulated hydraulic systems. Similarly, the undershoot and overshoot are decreased by using the adaptive PI controller, and this effect is highlighted when considering the fuzzy solution, with the most severe transients (*i.e.* start-up and shutdown). The fuzzy FTC approach, which directly compensates the fault effects, is always better than the adaptive PI method. In fact, the adaptive strategy, which relies on the on-line tracking of the controlled process, tries to compensate the faults by means of the iterative tuning of the PI parameters. The fuzzy FTC scheme neutralises any anomalous behaviour by estimating the fault signals and cancelling them out through the further control loop.

Finally, it is worth noting that when the safety-critical level of the process under diagnosis is relatively low, the straightforward implementation of redundant software sensing and control methodologies may be even cheaper and more reliable than the cheapest and simplest multiple redundant hardware sensor systems (Patton & Frank, 1989, 2000; Redmill an Anderson, 1996).

5. Conclusions

This paper proposes the design of two fault tolerant control schemes applied to a hydroelectric model in the Matlab and Simulink environments. The suggested fault tolerant controllers (adaptive and fuzzy) were used for regulating the speed of the Francis turbine of the hydraulic system. The nonlinear behaviour of the hydraulic turbine and the inelastic water hammer effects were considered in order to develop a high-fidelity simulator of this plant. The design strategies relying on estimation approaches were proposed for enhancing the derivation of the fault tolerant control methodologies. These features of the study represent a key point when on-line realisations are proposed for a viable application of the suggested fault tolerant control solutions. Moreover, the suggested design methodologies allowed to obtain the prescribed fault tolerance features of the controllers. The faults analysed in this paper affect the electric servomotor used as a governor, the hydraulic turbine speed sensor, and the hydraulic turbine itself. They are imposed both separately and simultaneously. Moreover, the complete drop of the rotational speed sensor is also analysed. Finally, the achieved capabilities of the suggested solutions were compared to those of a classical control scheme already implemented for the simulated hydroelectric system. Simulations on the hydroelectric plant model and the Monte-Carlo analysis were aimed at verifying the features of the considered control strategies, in the presence of parameter variations. The obtained results showed that the suggested design methodologies constitute viable and reliable approaches for application to real hydroelectric processes.

References

Alvisi, S., & Franchini, M. (2012). Grey neural networks for river stage forecasting with uncertainty. *Journal of Physics and Chemistry of the Earth*, *42–44*, 108–118. http://dx.doi.org/10.1016/j.pce.2011.04.002.

Asgari, H., Venturini, M., Chen, X., & Sainudiin, R. (2014). Modeling and simulation of the transient behavior of an industrial power plant gas turbine. *Journal of Engineering for Gas Turbines and Power*, *136*(6) 061601 (10 pp), http://dx.doi.org/10.1115/1.4026215.

Babuška, R. (1998). *Fuzzy modeling for control*. Kluwer Academic Publishers.

Blanke, M., Kinnaert, M., Lunze, J., & Staroswiecki, M. (2006). *Diagnosis and fault-tolerant control*. Berlin, Germany: Springer-Verlag.

Blesa, J., Rotondo, D., Puig, V., & Nejjari, F. (2014). FDI and FTC of wind turbines using the interval observer approach and virtual actuators/sensors. *Control Engineering Practice*, *24*, 138–155.

Bobál, V., Böhm, J., Fessl, J., & Machácek, J. (2005). *Digital self-tuning controllers: Algorithms, implementation and applications, advanced textbooks in control and signal processing* (1st ed.). Springer.

Please cite this article as: Simani, S., et al. Fault tolerant control of a simulated hydroelectric system. *Control Engineering Practice* (2016), http://dx.doi.org/10.1016/j.conengprac.2016.03.010

ARTICLE IN PRESS

Chen, J., & Patton, R. J. (1999). *Robust model-based fault diagnosis for dynamic systems*. Boston, MA, USA: Kluwer Academic Publishers.

Ding, S. X. (2008). *Model-based fault diagnosis techniques: Design schemes, algorithms, and tools* (1st ed.). Berlin Heidelberg: Springer ISBN: 978-3540763031.

Eker, I. (2004). Governors for hydro-turbine speed control in power generation: *A SIMO robust design approach*. *Energy Conversion and Management*, *45*(13–14), 2207–2221.

Fang, H., Chen, L., Dlakavu, N., & Shen, Z. (2008). Basic modeling and simulation tool for analysis of hydraulic transients in hydroelectric power plants. *IEEE Transactions on Energy Conversion*, *23*(3), 424–434.

Fonod, R., Henry, D., Charbonnel, C., Bornschlegl, E., Losa, D., & Bennani, S. (2015). Robust FDI for fault-tolerant thrust allocation with application to spacecraft rendezvous. *Control Engineering Practice*, *42*, 12–27.

Hanmandlu, M., & Goyal, H. (2008). Proposing a new advanced control technique for micro hydro power plants. *International Journal of Electrical Power & Energy Systems*, *30*(4), 272–282.

Hong, Y., Guangda, C., & Weiyou, C. (2008). Uncertain linear system D-domain robust stability fault tolerant control of hydraulic turbine regulator. In *The third international conference on electric utility deregulation and restructuring and power technologies—DRPT 2008*, http://dx.doi.org/10.1109/DRPT.2008.4523818.

Kiltz, L., Join, C., Mboup, M., & Rudolph, J. (2014). Fault-tolerant control based on algebraic derivative estimation applied on a magnetically supported plate. *Control Engineering Practice*, *26*, 107–115.

Kim, Y., & Kim, C. (2015). Modeling and response time analysis of the level 2 system for a continuous steel casting process. *Control Engineering Practice 44*, 117–125.

Kishor, N., Singh, S., & Raghuvanshi, A. (2006). Dynamic simulations of hydro turbine and its state estimation based lq control. *Energy Conversion and Management*, *47*(18–19), 3119–3137.

Kishor, N., Saini, R., & Singh, S. (2007). A review on hydropower plant models and control. *Renewable and Sustainable Energy Reviews*, *11*(5), 776–796.

Kulhavý, R. (1987). Restricted exponential forgetting in real-time identification. *Automatica*, *23*(9), 589–600.

Li, Z., Ye, L., Wei, S., Malik, O. P., Hope, G. S., & Hancock, G. C. (1992). Fault tolerance aspects of a highly reliable microprocessor-based water turbine governor. *IEEE Transactions on Energy Conversion*, *7*(1), 1–7. http://dx.doi.org/10.1109/60.124534.

Li, Y., Liu, F., & Cao, Y. (2015). Delay-dependent wide-area damping control for stability enhancement of HVDC/AC interconnected power systems. *Control Engineering Practice*, *37*, 43–54.

Ljung, L. (1999). *System identification: Theory for the user* (2nd ed.). Englewood Cliffs, NJ: Prentice Hall.

Mahmoud, M., Dutton, K., & Denman, M. (2005). Design and simulation of a non-linear fuzzy controller for a hydropower plant. *Electric Power Systems Research*, *73*(2), 87–99.

Mansoor, S., Jones, D., Bradley, D., Aris, F., & Jones, G. (2000). Reproducing oscillatory behaviour of a hydroelectric power station by computer simulation. *Control Engineering Practice*, *8*(11), 1261–1272.

Nelles, O. (2001). *Nonlinear system identification*. Berlin Heidelberg, Germany: Springer-Verlag.

Noura, H., Theilliol, D., Ponsart, J.-C., & Chamseddine, A. (2009). *Fault-tolerant control systems: Design and practical applications advances in industrial control* (1st ed.). London: Springer.

Patton, R.J., Frank, P.M., & Clark R.N. (Eds.). (1989). *Fault diagnosis in dynamic systems, theory and application, control engineering series*. London: Prentice Hall,.

Patton, R.J., Frank, P.M., & Clark, R.N. (Eds.). (2000). Issues of Fault diagnosis for dynamic systems. Springer-Verlag, London Limited.

Patton, R.J., Simani, S., Daley, S., & Pike, A. (2000). Fault diagnosis of a simulated model of an industrial gas turbine prototype using identification techniques. In *The fourth symposium on fault detection supervision and safety for technical processes*, *SAFEPROCESS2000* (Vol. 1, pp. 518–524), Budapest, Hungary.

Redmill, F., & Anderson, T. (Eds.). (1996). *Safety-critical systems: The convergence of high tech and human factors*, 1st ed. Leeds, UK: Springer. ISBN:978-3540760092.

Schuh, M., Zgorzelski, M., & Lunze, J. (2015). Experimental evaluation of an active fault-tolerant control method. *Control Engineering Practice*, *43*, 1–11.

Simani, S., & Castaldi, P. (2013). Data-driven and adaptive control applications to a wind turbine benchmark model. *Control Engineering Practice*, *21*(12), 1678–1693. http://dx.doi.org/10.1016/j.conengprac.2013.08.009 (Special issue invited paper). ISSN: 0967-0661. PII: S0967-0661(13)00155-X..

Simani, S., Fantuzzi, C., Rovatti, R., & Beghelli, S. (1999). Parameter identification for piecewise linear fuzzy models in noisy environment. *International Journal of Approximate Reasoning*, *1*(22), 149–167.

Simani, S., Alvisi, S., & Venturini, M. (2014). Study of the time response of a simulated hydroelectric system. *Journal of Physics: Conference Series 570*, 1–13. ISSN: 1742-6596. http://dx.doi.org/10.1088/1742-6596/570/5/052003.

Simani, S., Farsoni, S., & Castaldi, P. (2014). Fault diagnosis of a wind turbine benchmark via identified fuzzy models. *IEEE Transactions on Industrial Electronics*, *62*(6), 3775–3782. http://dx.doi.org/10.1109/TIE.2014.2364548 (Invited paper for the special issue "Real-time fault diagnosis and fault tolerant control).

Simani, S., Alvisi, S., & Venturini, M. (2015). Data-driven design of a fault tolerant fuzzy controller for a simulated hydroelectric system. In IFAC (Ed.), *Proceedings of the ninth IFAC symposium on fault detection, supervision and safety for technical processes—SAFEPROCESS'15*, IFAC, Paris, France (Special session invited paper).

Takagi, T., & Sugeno, M. (1985). Fuzzy identification of systems and its application to modeling and control. *IEEE Transaction on System, Man and Cybernetics*, *SMC-15*(1), 116–132.

Ubaid, U., Daley, S., & Pope, S. A. (2015). Design of remotely located and multi-loop vibration controllers using a sequential loop closing approach. *Control Engineering Practice*, *38*, 1–10.

Weber, H., Prillwitz, F., Hladky, M., & Asal, H.-P. (2001). Reality oriented simulation models of power plants for restoration studies. *Control Engineering Practice*, *9*(7), 805–811.

Wei, L., Wei-bo, L., Gen-mao, W., & Jian-hua, W. (2000). Research on the methods of detecting and removing slide valve failure. *Journal of Zhejiang University Science*, *1*(1), 56–60.

Zhang, Y., & Jiang, J. (2008). Bibliographical review on reconfigurable fault-tolerant control systems. *Annual Reviews in Control*, *32*, 229–252.

UNCORRECTED PROOF

Please cite this article as: Simani, S., et al. Fault tolerant control of a simulated hydroelectric system. *Control Engineering Practice* (2016), http://dx.doi.org/10.1016/j.conengprac.2016.03.010